sciendo

RIGA TECHNICAL
UNIVERSITY

Theoretical Foundations of Gas Hydrate Synthesis Intensification

Bogdan KUTNYI[1], Anatoliy PAVLENKO[2*], Oleksandra CHEREDNIKOVA[3]

[1,3]*Department of Heat and Gas Supply, Ventilation and Heating, National University «Yuri Kondratyuk Poltava Polytechnic», Poltava, Ukraine*

[2]*Department of Building Physics and Renewable Energy, Kielce University of Technology, Kielce, Poland*

Abstract** – **The methods of industrial production of gas hydrates are considered, their problems are identified, and a list of factors that are decisive for the intensification of mass exchange processes is outlined. The prospective use of mass transfer devices with a dynamic interfacial surface for the synthesis of gas hydrates is substantiated. A mathematical model of hydrate formation on the surface of a water droplet moving in a gas flow is proposed. Digital solutions for various droplet sizes, velocities, gas pressures, water temperature, gas permeability of gas hydrate, and dynamics of hydrate formation over time were obtained. It was established that the main ways of intensification of the synthesis of gas hydrates are: obtaining smaller water droplets, maintaining the gas temperature at the level of 0 °C, increasing the gas pressure, and increasing the residence time of the droplet in the gas medium. Approximation formulas for calculating quantitative indicators of the influence of various factors on the formation of methane gas hydrate have been obtained. The analysis of the obtained results made it possible to establish promising directions for the optimization of equipment for the synthesis of gas hydrates.

Keywords** – **Gas hydrates; heat exchange; industrial synthesis; installations; mass exchange.

1. INTRODUCTION

Gas hydrates (GH) have great prospects for application in various industries and the national economy [1]. However, they are not widely used now because industrial technologies for their synthesis are not sufficiently developed. Known installations for GH synthesis have a number of disadvantages: low rate of mass exchange processes, formation of gas hydrates with a high concentration of water, complex structures and high cost [2]. When calculating and designing mass transfer devices for the industrial synthesis of GH, the task of intensification of mass transfer processes is extremely important.

The most promising ways to solve this problem are: optimization of the thermobaric conditions of hydrate formation, increasing the area of the interphase surface and effective removal of heat from the region of hydrate formation [3], [4]. Solving these questions experimentally has high reliability, but requires a lot of time and money. Therefore, in order to outline promising directions of research in this paper, the methods of mathematical modelling of hydrate formation processes are applied.

* Corresponding author.
E-mail address: apavlenko@tu.kielce.pl

2. ANALYSIS OF LITERATURE DATA AND PROBLEM STATEMENT

In most cases, issues of intensification of mass transfer processes arise at the design stage or immediately after the commissioning of another installation for the synthesis of gas hydrates. A number of authors choose thermobaric conditions, some use surface-active substances, and make structural changes, which are usually aimed at increasing the area of the interfacial surface and increasing the time of its active functioning [5], [6].

The result of these works is usually a set of experimental data, which are statistically processed and based on this, empirical dependencies are derived [7]. The main drawback of such empirical formulas is 'tying' to the specific conditions of conducting experiments on the installation of a certain structure with one or another gas. Of course, on the basis of these data, in a first approximation, certain generalizing trends of the influence of various factors on the process of hydrate formation can be deduced, but it is impossible to guarantee their quantitative influence in other conditions without mathematical modelling.

For the industrial synthesis of GH, devices with a dynamic phase contact surface are the most promising [8]. Peculiarities of hydrate formation in bubbling devices are considered in works [9], [10]. Therefore, in this article, we will focus on the study of the influence of various factors on the intensification of hydrate formation in injection installations.

3. THE PURPOSE AND TASKS OF THE RESEARCH

The purpose of this work is to determine the directions of intensification of mass transfer processes by optimizing the design features and operating modes of installations for the synthesis of GH. In the synthesis of GH, two processes simultaneously take part: the removal of heat from the interphase surface and the supply of gas to this surface. To obtain the maximum rate of hydrate formation, these two processes must be balanced – this is the first condition.

In the process of hydrogenesis, a GH crust is formed on the interfacial surface of liquid droplets, which has heat-insulating and sealing properties. Therefore, it is necessary to take into account the development of heat and mass transfer processes in time. This is the second important factor that slows down the process of hydroformation.

The third factor is the hydrodynamics of the interphase surface, which depends on the design features of this or that device. The process of hydrate formation can occur on the surface of a liquid, on the surface of liquid drops, on the surface of ice and GH crystals, on the surface of oscillating gas bubbles, etc. As a rule, the intensity of heat and mass exchange processes is expressed through criterion equations obtained experimentally. The analysis of known data shows that only two methods of hydrate formation have the highest velocities: on the surface of water droplets in the gas flow; on the surface of gas bubbles in the liquid volume. This work is devoted to the study of hydrate formation on the surface of a water droplet moving in a gas flow.

In [11], the kinetics of CO_2 hydrate formation was considered. The authors note a significant unevenness in the rate of hydrate formation and make assumptions about the cause of this phenomenon. According to the authors, the main role in this process is played by the GH crust, which forms on the interphase surface and significantly slows down the flow of gas to it.

The task of this paper is to quantitatively assess the influence of various factors on the process of hydrate formation, which occurs on the surface of a water droplet moving in a gas stream. Mathematical modelling of hydrate formation in various hydrodynamic and

thermobaric conditions is a tool for researching heat and mass transfer processes on the interphase surface.

4. PRESENTATION OF THE MAIN MATERIAL

Mathematical model of heat and mass transfer processes at the interphase surface. Let's consider the physical model of the process of hydrate formation on the water surface, considering the thickness of the GH crust (δ_{gh}) three to four orders of magnitude smaller than the size of a droplet of water, Fig. 1. For the formation of GH, it is necessary to remove heat (q_1) to the gaseous medium and to the liquid (q_2). Since GH is actually a heat insulator, after the GH crust is formed, the heat transfer resistance increases (δ_{gh}/λ_{gh}). At the same time, mass transfer resistance increases (δ_{gh}/σ_{gh}), because the gas hydrate crust is poorly permeable to gas. The thickness of the crust depends on the intensity of mass transfer (m_g) and time (τ).
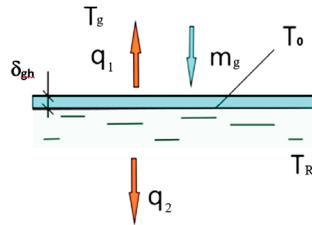
Fig. 1. Scheme of heat and mass flows near the interphase surface. q_1 – specific heat flow with diffusing gas; q_2 – specific heat flow into the liquid; m_g – specific mass flow of gas.

To calculate hydrate formation on the interphase surface, the system of heat and mass transfer Eq. (1) can be applied, which consists of the equation of heat flows between the surface of the droplet, the gas (q_1) and liquid (q_2); heat transfer equation from the process of hydrate formation (q_3); equation for determining the temperature regime of water in a droplet (T_w); the equation for determining the mass transfer coefficient near the interphase surface (β); equation for determining the mass of gas used to form gas hydrate (m_g); differential equation for determining the thickness of the gas hydrate crust (δ_{gh}). Avoiding the formation of ice both on the interfacial surface and in the volume of the droplet is also an important condition.

$$q_3 = q_1 + q_2 \tag{1}$$

$$q_1 = \frac{T_0 - T_g}{\dfrac{1}{a_1} + \dfrac{\delta_{gh}}{\lambda_{gh}}} \tag{2}$$

$$q_2 = k_2(T_0 - T_w) \tag{3}$$

$$q_3 = \frac{m_g \cdot r_{gh}}{\overline{m}_{gh}} \tag{4}$$

$$\frac{m_w c_w}{\pi D^2} \frac{dT_w}{d\tau} = k_2(T_0 - T_w) \tag{5}$$

$$\beta = \frac{\text{Nu'}}{\text{Nu}} \frac{D_g \alpha_1}{\lambda_g}, \tag{6}$$

$$m_g = \frac{\rho_g - \rho_0}{\dfrac{1}{\beta} - \dfrac{\delta_{gh}}{\sigma_{gh}}} \tag{7}$$

$$\frac{d\delta_{gh}}{d\tau} = \frac{m_g}{\overline{m}_{gh} \rho_{gh}} \tag{8}$$

$$T_0 \geq 273.15, K; T_w \geq 273.15, K, \tag{9}$$

where

q Specific heat flux, W/m^2;

T_0, ρ_0 Temperature and gas density at the line of hydrate formation, K and kg/m^3;

T_g, ρ_g Temperature and density of gas in the device, K and kg/m^3;

α_1 Heat exchange coefficient near the interphase surface from the side of the gas phase, W/(m^2·K);

k_2 Heat transfer coefficient through the layer of the spherical surface from the liquid side, W/(m^2·K);

T_w Liquid temperature, K;

m_w Mass of water in a droplet, kg;

c_w Heat capacity of water, J/(kg·°C);

D Droplet diameter, m;

δ_{gh} Gas hydrate crust thickness, m;

σ_{gh} Gas permeability of gas hydrate crust, m^2/s;

λ_{gh} Coefficient of thermal conductivity GH, W/(m·K);

m_g Specific mass flow, kg/(s·m^2);

β Mass transfer coefficient, m/s;

r_{gh} Heat of dissociation of GH, J/kg;

Nu, Nu'   Heat exchange and diffusion Nusselt criteria;

D_g Molecular diffusion coefficient, m^2/s;

λ_g Gas thermal conductivity coefficient, W/(m·K).

In literary sources [12]–[14], several options for determining the gas permeability of the gas hydrate crust are given, and it has different units of measurement (for example, m^2, m^2/(s·Pa), m^2/s). In our case, the gas permeability of the gas hydrate has the same dimension as the diffusion coefficient. Actually, this is consistent with known literary sources [14], however, due to the lack of reliable data, it is necessary to take into account approximate numerical values of this parameter ($5\cdot10^{-16} < \sigma_{gh} < 5\cdot10^{-14}$ m^2/s).

Heat transfer coefficients near the interphase surface can be determined using criterion equations, of the form:

$$\text{Nu} = f(\text{Re}, \text{Pr}), \tag{10}$$

where

Nu   Nusselt criterion;

Re   Reynolds criterion;

Pr   Prandtl's criterion.

In various nozzle chambers, humidifying devices that are widely used in refrigeration equipment, heat and mass exchange occurs between water droplets and a gas medium [7], [15]. Similarity equations are used to calculate heat and mass transfer coefficients:

$$\mathrm{Nu} = 2.0 + 0.6\,\mathrm{Re}^{0.6}\,\mathrm{Pr}^{0.33}\,, \tag{11}$$

$$\mathrm{Nu'} = 2.0 + 0.6\,\mathrm{Re}^{0.5}\,\mathrm{Pr}_\mathrm{d}^{0.33}\,. \tag{12}$$

These equations can be applied in the range $0 < \mathrm{Re} < 1000$, which is enough to perform calculations in the field of hydrate formation. To find the difference in densities ($\rho_\mathrm{g}-\rho_0$), express the gas density in terms of pressure and temperature from the equation of thermodynamic state

$$\rho = \frac{P\mu_\mathrm{g}}{R_\mu TZ}\,, \tag{13}$$

where
P Pressure, Pa;
μ_g Molecular mass of gas, kg/mol;
R_μ Universal gas constant, J/(mol·K);
T Gas temperature, K;
Z Gas compressibility coefficient.

Taking into account Eq. (13), the difference in densities from the system of Eq. (1) can be determined through the difference in thermobaric parameters, kg/m^3

$$\rho_\mathrm{g} - \rho_0 = \frac{\mu_\mathrm{g}}{R_\mu}\left(\frac{P_\mathrm{g}}{T_\mathrm{g}Z_\mathrm{g}} - \frac{P_0}{T_0 Z_0} \right)\,, \tag{14}$$

where P_g and P_0 – are gas pressures, respectively, in the apparatus and near the interphase surface where the process of synthesis of GH, Pa occurs.

To use Eq. (14), it is necessary to determine the compressibility factor (Z). Known methods of calculating the compressibility coefficient have been developed and standardized for natural gas of different composition [16]. Analysis of the operation of various equations of state in a wide range of pressures and temperatures shows that in the range of thermobaric conditions of hydrate formation, the Soave-Redlich-Kwong modification can be applied with an accuracy of up to 5 % [17], [18].

Gas compressibility coefficient

$$Z_\mathrm{g} = \frac{V_\mathrm{g}}{V_\mathrm{g} - b_\mathrm{g}} - \frac{1}{3\left(\sqrt[3]{2}-1\right)^2}\frac{b_\mathrm{g}}{V_\mathrm{g} + b_\mathrm{g}}F_{(\mathrm{g})}\,, \tag{15}$$

where
V_g Molar volume;
b_g Constant value;
$F_{(\mathrm{g})}$ Modifying function.

The molar volume of the gas is found from the formula (16):

$$V_g = \frac{\mu_g}{\rho_g}. \tag{16}$$

The constant b_g can be determined from the known thermodynamic parameters of this gas at the critical point

$$b_g = \frac{\sqrt[3]{2}-1}{3}\frac{R_\mu T_{kg}}{P_{kg}}, \tag{17}$$

where T_{kg} – gas temperature at the critical point, K and P_{kg} – gas pressure at the critical point, Pa. The modifying function is determined using the Soave equation [15]:

$$F_{(g)} = \frac{T_{kg}}{T}\left\{1+\left(0.48+1.574\omega_g-0.17\omega_g^2\right)\left(1-\sqrt{\frac{T}{T_{kg}}}\right)\right\}, \tag{18}$$

where ω_g – acentric factor. Gas acentric factors are given in [19].

If the pressure and temperature of the gas in the apparatus can be set, then at the interphase surface these parameters are connected to each other by the line of hydrate formation. For various gases, the hydrate formation pressure [20], [21] can be determined using the empirical equation, Table 1.

TABLE 1. APPROXIMATE FORMULAS FOR DETERMINING THE HYDRATE FORMATION PRESSURE ON THE EQUILIBRIUM LINE

Hydrate-forming gas	Temperature range, °C	Pressure of the equilibrium state of the hydrate, Pa, °C
1	2	3
Methane	$0 < t_0 < 22.0$	$P_0 = 10^{\{6+0.006(18+t0)1.5\}}$
Carbon dioxide	$0 < t_0 < 10$	$P_0 = 10^{\{6.01+0.05t0\}}$
Hydrogen sulfide	$0 < t_0 < 29$	$P_0 = 10^{\{5+0.045t0\}}$
Propane	$0 < t_0 < 5.5$	$P_0 = 10^{\{5.24+0.093t0\}}$
Ethan	$0 < t_0 < 14.5$	$P_0 = 10^{\{5.72+0.0555t0\}}$

Note: t_0 – gas hydrate formation temperature, °C; P_0 – absolute equilibrium pressure on the line of gas hydrate formation, Pa.

The Nusselt criteria in the system of Eq. (1) depends on the method of organizing heat and mass transfer processes near the interphase surface, which in turn are determined mainly by the design features of a specific mass transfer device. Comparing Eq. (10) and (11) we see that the ratio of diffusion and heat exchange Nusselt criteria will be close to unity. This actually follows from the theory of similarity of heat exchange and mass exchange processes [22]. Thus, as the most common option in most processes, the value can be taken:

$$\frac{\mathrm{Nu}'}{\mathrm{Nu}} \approx 1. \tag{19}$$

The Reynolds criterion in Eq. (11), and Eq. (12) is determined by the mutual velocity of the liquid droplet and the gas flow in which it resides. As a rule, the initial speed difference is

maximal, and the final speed difference is equal to the hovering speed. Therefore, the difference in the velocity of the droplet and the gas flow will have a variable character and will be described by the formula:

$$\frac{\mathrm{d}V}{\mathrm{d}\tau} = -a \,, \tag{20}$$

where a is the acceleration of the movement, which is directed in the direction opposite to the speed, m/s^2. This acceleration is a consequence of the balance of inertia forces and resistance of the environment. For spherical particles in a wide range of movement speeds, the acceleration can be found from the formula, m/s^2

$$a = \frac{3}{4} \frac{C}{D} \frac{\rho_\mathrm{g}}{\rho_\mathrm{w} - \rho_\mathrm{g}} V^2, \tag{21}$$

where C is the aerodynamic coefficient, which for different modes of movement acquires the following values:

$$\text{Laiminar mode Re<0.2;} \quad C = \frac{24}{\mathrm{Re}}, \tag{22}$$

$$\text{Transitional area } 0.2 < \mathrm{Re} < 500; \quad C = \frac{18.5}{\mathrm{Re}^{0.6}}, \tag{23}$$

$$\text{Turbulent mode Re} > 500; \quad C = 0.44 \,. \tag{24}$$

Since the size of the drops can vary widely, we determine the floating speed by the Eq. (21), taking into account that $a = g$

$$V_\mathrm{s} = \sqrt{\frac{4gD\left(\rho_\mathrm{w} - \rho_\mathrm{g}\right)}{3C\rho_\mathrm{g}}} \,. \tag{25}$$

Thus, the equation of motion of a droplet is described by the dependence

$$\frac{\mathrm{d}V}{\mathrm{d}\tau} = \frac{3C\rho_\mathrm{g}}{4D\left(\rho_\mathrm{w} - \rho_\mathrm{g}\right)} V^2 \,. \tag{26}$$

Together with Eq. (11), we get the time-varying heat transfer coefficient on the surface of the droplet.

The water inside the droplet can be considered stationary. Therefore, the process of heat transfer is reduced only to thermal conductivity in the sphere. Applying Fourier's law of heat conduction, the amount of heat transferred through a spherical wall, W

$$Q = -\lambda_\mathrm{w} F \frac{\mathrm{d}t_\mathrm{w}}{\mathrm{d}r} = -\lambda_\mathrm{w} \pi D^2 \frac{\mathrm{d}t_\mathrm{w}}{\mathrm{d}r} \,. \tag{27}$$

Integrating this equation gives the well-known expression, W

$$Q = \pi \lambda_\mathrm{w} d_1 d_2 \frac{t_\mathrm{w1} - t_\mathrm{w2}}{\delta} = \frac{\lambda_\mathrm{w}}{\delta} \frac{d_2}{d_1} F(t_\mathrm{w1} - t_\mathrm{w2}) \,, \tag{28}$$

where d_1 – outer diameter of the droplet ($d_1 = D$), m and d_2 – conditional diameter of the sphere on the surface of which the entire mass of the droplet is concentrated, m. Thus, the coefficient of equivalent heat transfer, W/(m²·°C)

$$k_2 = \frac{\lambda_w}{\delta} \frac{d_2}{D}. \tag{29}$$

Considering the volume of the droplet divided into 2 parts, which have the same mass, it can be written, kg

$$m_1 = v_1 \rho_w = \frac{4}{3} \pi r_1^3 \rho_w,$$
$$m_2 = v_2 \rho_w = \frac{4}{3} \pi r_2^3 \rho_w. \tag{30}$$

Since $m_2 = m_1/2$ we can determine the radius of the conditional sphere, m

$$r_2 = \frac{r_1}{\sqrt[3]{2}},$$
$$d_2 = \frac{D}{\sqrt[3]{2}}. \tag{31}$$

After substituting d_2 from Eq. (31) into Eq. (29), will be obtained, W/(m²·°C)

$$k_2 = \frac{\lambda_w}{\delta} \frac{1}{\sqrt[3]{2}}. \tag{32}$$

The thickness of the heat-conducting wall, m

$$\delta = r_1 - r_2 = r_1 \left(1 - \frac{1}{\sqrt[3]{2}} \right) \tag{33}$$

After substituting Eq. (33) into Eq. (32), we obtain, W/(m²·°C)

$$k_2 = \frac{\lambda_w}{r_1 \left(\sqrt[3]{2} - 1 \right)} = \frac{2\lambda_w}{D \left(\sqrt[3]{2} - 1 \right)} \tag{34}$$

After substituting Eq. (33) into Eq. (32), we obtain, W/(m²·°C)

$$k_2 \approx \frac{\lambda_w}{0.13D} \tag{35}$$

The temperature of the water in the droplet also changes over time. In particular, a droplet of liquid in the gas phase will be gradually heated by the heat of the hydrate formation process. The temperature regime of the droplet can be recorded using its 'point' model:

$$\frac{dT_w}{d\tau} = \frac{\alpha_2 \pi D^2}{m_w c_w} \left(T_0 - T_w \right). \tag{36}$$

Whence, after substituting k_2 from Eq. (34), we obtain

$$\frac{dT_w}{d\tau} = \frac{2\lambda_w \pi D^2}{\frac{1}{6}\pi D^3 \rho_w c_w \left(\sqrt[3]{2}-1\right)D}\left(T_0 - T_w\right).$$ (37)

After reductions, we obtain from Eq. (37)

$$\frac{dT_w}{d\tau} = \frac{12\lambda_w}{D^2 \rho_w C_w \left(\sqrt[3]{2}-1\right)}\left(T_0 - T_w\right) \approx \frac{46.17\lambda_w}{D^2 \rho_w C_w}\left(T_0 - T_w\right).$$ (38)

Taking into account Eqs. (10)–(38), the system of Eq. (1) for methane takes the form Eqs. (39)–(46). It can be used not only to analyse the intensity of hydrate formation in various thermobaric conditions, but also to study the dynamics of processes over time.

$$\frac{dV}{d\tau} = -\frac{3V\rho_g}{4D(\rho_w - \rho_g)}V^2$$ (39)

$$\alpha_1 = \frac{\lambda_g}{D}\left(2.0 + 0.6\left(\frac{VD}{V_g}\right)^{0.5}Pr^{0.33}\right)$$ (40)

$$T_0 = T_g + \left(\frac{m_g r_{gh}}{\overline{m}_{gh}} - \frac{\lambda_w}{0.13D}\left(T_0 - T_w\right)\right)\left|\frac{1}{\alpha_1} + \frac{\delta_{gh}}{\lambda_{gh}}\right|$$ (41)

$$\frac{dT_w}{d\tau} = \frac{46.17\lambda_w}{\rho_w C_w D^2}\left(T_0 - T_w\right)$$ (42)

$$P_0 = 10^{\left\{6+0.006\left(T_0 - 255.15\right)^{1.5}\right\}}$$ (43)

$$m_g = \frac{1}{\frac{\lambda_g}{\alpha_1 D_g} + \frac{\delta_{gh}}{\sigma_{gh}}}\frac{\mu_g}{R_\mu}\left\{\frac{P_g}{T_g Z_g} - \frac{P_0}{T_0 Z_0}\right\}$$ (44)

$$\frac{d\delta_{gh}}{d\tau} = \frac{m_g}{\overline{m}_{gh}\rho_{gh}}$$ (45)

$$T_0 \geq 273.15, K; \; T_w \geq 273.15, K$$ (46)

A computer program S*yntez* was developed to perform mathematical modelling. The system of differential equations of the first order is solved by the Runge-Kutta method of the 4th order. The experimentally determined time step depends on the droplet diameter and thermobaric conditions and can vary within the limits 10^{-10}–10^{-5} sec.

5. RESULTS OF EXPERIMENTAL STUDIES OF MASS TRANSFER AT THE INTERPHASE SURFACE

Let's highlight a set of factors that can potentially have a significant impact on the process of hydrate formation: droplet size; the influence of the area of speed gain (acceleration) and the speed of the droplet; water droplet temperature; gas temperature, especially its decrease; gas permeability of gas hydrate; gas pressure.

With the hydraulic method of spraying, it is possible to obtain an aerosol with a dispersion of 30 to 500 microns. The dispersion of the aerosol with the pneumatic method of spraying is within 50–200 µm [23]–[26]. Therefore, in further calculations, the droplet range of 30–500 µm is accepted.

The output data for the calculation are as follows: λ_{gh} = 0.5 W/(m·K); σ_{gh} = (5–10)$^{-14}$ m^2/s; = 0.129; ρ_{gh} = 913 kg/m^3; r_{gh} = 3060 kJ/kg; λ_g = 0.031 W/(m·K); μ_g = 0.016 kg/mol; P_{rg} = 0.734; T_{kg} = 190.66 °K; P_{kg} = 4.64 MPa; ω_g = 0.0101; c_w = 4187 J/(kg·K).

5.1. The Speed of the Droplet

The mutual initial speed of the droplet in the gas phase is determined by the design features of the nozzles and the pressure of the medium supplied to the nozzle. For different types of nozzles, the most common speeds are in the range of 10÷100 m/s. Initial conditions: temperature t_w = +5 °C, t_g = +0 °C; gas pressure P_g = 4.9 MPa. The calculation results were used to draw graphs: the dynamics of the speed of drops of different sizes, Fig. 2; speed of floating drops, Fig. 3; intensity of mass transfer on the interphase surface, Fig. 4.

The analysis of the obtained results in Fig. 2 shows that, regardless of the initial gas velocity, the duration of the droplet acceleration section depends mainly on their size and is 10^{-5}–10^{-4} s. With an initial speed difference of 100 m/s, drops of different sizes will be able to fly a distance of 0.01–0.1 mm during this time. Due to the short duration, the accelerating parts of the droplet motion and the initial gas velocity have practically no effect on the amount of synthesized GH. The main part of the droplet movement, on which the gas hydrate is accumulated, occurs at the speed of soaring, Fig. 3.
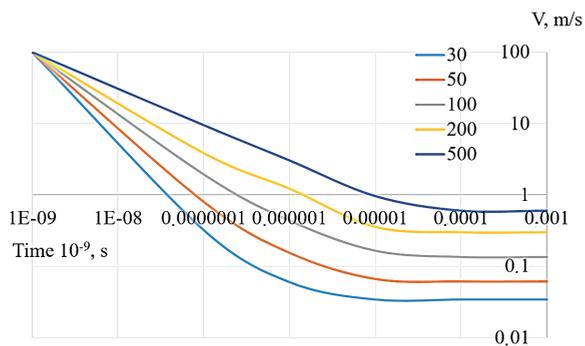
Fig. 2. Dynamics of the difference in speed of water droplets with sizes in the range of 30÷500 µm relative to the gas phase (at a gas speed of 100 m/s).
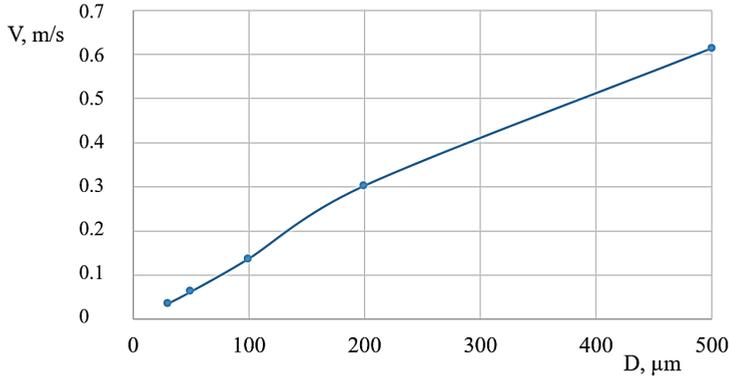
Fig. 3. The floating speed (V) of water drops with a diameter of D in methane for a pressure of 4.9 MPa.

The results of calculating the intensity of mass transfer on the surface of drops of different sizes were obtained for the initial section of their movement at the temperature of gas and water +5 °C (Fig. 4). Analysis of the dynamics of hydrate formation shows a significant intensification of mass exchange processes in the time interval of up to 0.1 s for drops with a diameter of up to 100 µm and more than 1 s for drops with a size of 200–500 µm. This effect corresponds to the period of heating of the droplet by the heat released during the formation of gas hydrate, which leads to an increase in the temperature of the droplet by 1.5–2 °C. It is difficult to increase the intensity of hydrate formation by lowering the initial water temperature, as there is a danger of freezing. Another possible way is to reduce the gas temperature.

5.2. Droplet Size

The influence of the size of water droplets on the amount of gas hydrate was studied (V_d) for different droplet sizes (in the range of 0.03–0.5 mm) at a gas pressure of 4.9 MPa. The total area of droplets of a given size for a constant volume of liquid is taken into account.
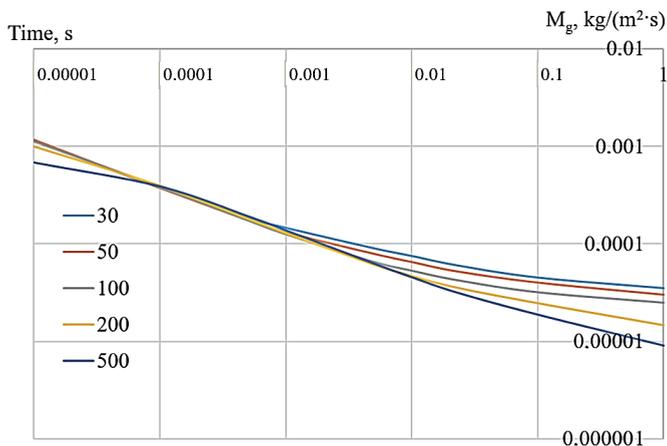
Fig. 4. The dynamics of mass transfer intensity (M_g) on the surface of drops of different sizes (30, 50, 100, 200 and 500 µm).

The results of the calculation of hydrate formation for a constant volume of water and in comparison, with droplets of size 500 μm (V_{500}) are shown in Fig. 5. The advantage of using droplets of minimum size in devices for the industrial production of gas hydrates is obvious. This dependence (Fig. 5) can be described by an approximation curve:

$$V_d = 0.515 \frac{V_{500}}{D^{0.941}}, \tag{47}$$

where *D* is the droplet size, mm. The obtained results indicate that the decrease in the droplet size allows increasing the amount of obtained gas hydrate almost proportionally.

5.3. Time

The thickness of the GH crust on the surface of the droplet increases over time, but due to the slowing down of mass transfer processes (Fig. 4), the growth of the GH crust thickness also slows down. The change in the thickness of the GH crust over time for droplets with a diameter of 500 μm, at a gas pressure of 4.9 MPa, a gas temperature of 0 °C and a water temperature of +5 °C, can be approximated by the equation, mm

$$\delta_{gh} = \frac{\tau^{0.6}}{10^4}, \tag{48}$$

where τ – time, s. The obtained results show that the process of GH synthesis must be organized in such a way that the duration of phase contact is as long as possible.

5.4. Gas Temperature

The next important factor for the intensification of the industrial synthesis of GH is the gas temperature – the lower it is, the faster GH will be formed. However, over time, conditions arise when the intensity of mass transfer will decrease to such an extent that freezing of the droplet will begin. Mathematical modelling was performed to study these processes.
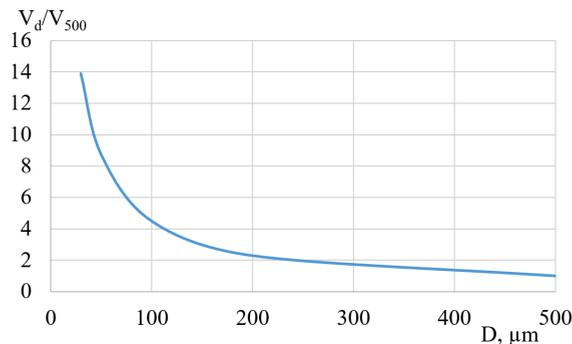
Fig. 5. Relative intensity of hydrate formation depending on the size of liquid drops (*D*).

The initial temperature of the water is taken as constant $t_w = +5$ °C. The studied gas temperature varied within the limits $t_g = -15 - +5$ °C. The calculation results are shown in Fig. 6. The analysis of the obtained results shows that the optimal temperature for hydrate formation is a gas temperature equal to 0 °C. Under the conditions of negative gas

temperatures, the intensity of hydrogenesis increases, however, freezing of water droplets occurs and the thickness of the GH crust remains less than under optimal conditions. An increase in gas temperature also leads to a slowdown in mass processes, and the thickness of the GH crust also rapidly decreases, Fig. 6.

Analysis of the application of negative gas temperatures, Fig. 7, shows that freezing of liquid drops occurs in less than 0.05 s. And only for drops of a relatively large size, icing is observed within 0.05–0.2 s. With such rapid freezing of liquid droplets, the process of hydrate formation slows down even before the GH crust reaches a significant thickness, Fig. 6. Since the real jet contains drops of different sizes and, above all, small drops, the use of gas with negative temperatures cannot be considered promising.
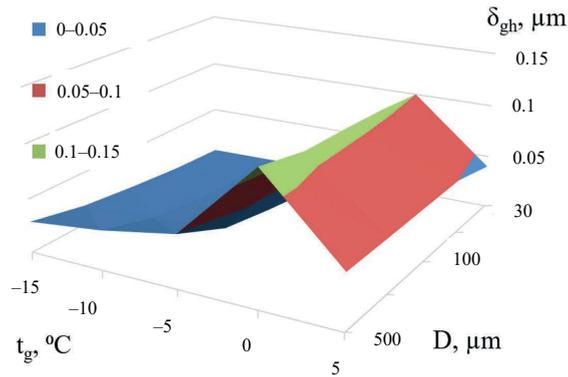
Fig. 6. GH crust thickness (δ_{gh}) depending on gas temperature (t_g) and liquid droplet size (D).
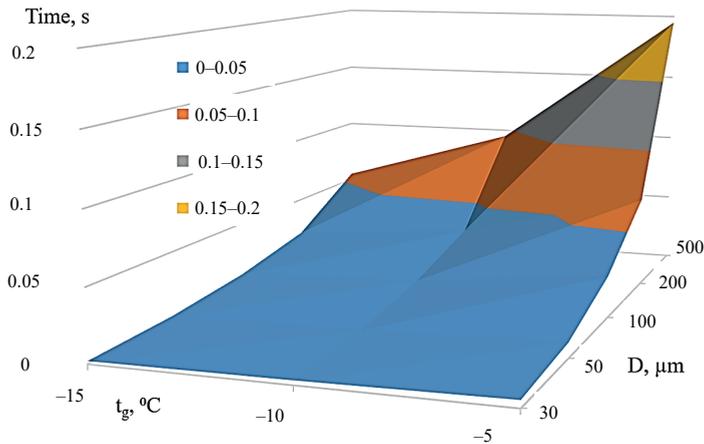
Fig. 7. Freezing time of droplets of different sizes in a gas flow with different temperatures.

5.5. Gas Permeability of Gas Hydrate

In order to assess the influence of the gas permeability of the GH crust on its thickness, calculation studies of the formation of GH at different values of gas permeability were carried out (σ): $5 \cdot 10^{-14}$, $5 \cdot 10^{-15}$ and $5 \cdot 10^{-16}$ m^2/s. The thickness of the GH crust is taken as the 'base' value (δ_{14}), which is formed on the surface of the droplet when the gas permeability of GH is at the level $\sigma = 5 \cdot 10^{-14}$. The results of the performed calculations are shown in Fig. 8.

Approximation of dependence shown in Fig. 8 has the form

$$\delta_{gh} = 3{\cdot}10^6 \delta_{14}\sigma^{0.4869} . \tag{49}$$

The obtained results convincingly prove that a decrease in gas permeability leads to a significant decrease in the amount of formed GH. Therefore, further clarification of the gas permeability of GH is necessary, which requires additional experimental studies.
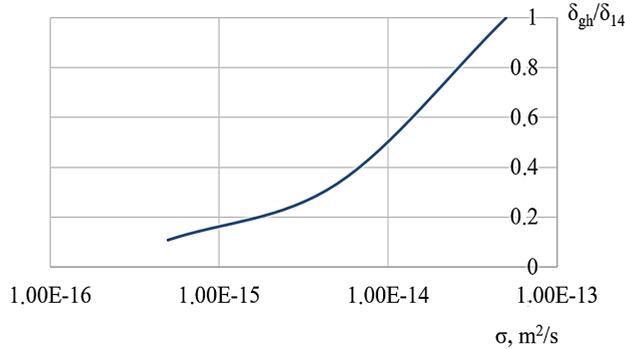
Fig. 8. The effect of gas permeability of GH on the thickness of the GH crust on the surface of the droplet.

5.6. Gas Pressure

The fourth important factor in hydrate formation is gas pressure. In order to establish the quantitative characteristics of this influence, a number of calculations were performed. Initial data: initial water temperature +5 °C; gas temperature 0 °C; droplet size range 30–500 μm.; gas pressure range 4.9–10 MPa; gas speed 20 m/s. The results of calculating the thickness of the GH crust, which forms on the surface of a droplet of water in 0.01 s, are shown in Fig. 9.

The analysis of the obtained results shows that for different droplet sizes, the intensification of heat exchange occurs almost equally. A two-fold increase in pressure makes it possible to increase the rate of synthesis of methane gas by approximately 2–2.5 times. Within the range of pressures from 4.9 to 10 MPa, an approximate dependence of the form was obtained

$$\frac{\delta_{gh}}{\delta_{gh(P=4.9)}} = 0.3929P - 0.8929 . \tag{50}$$

where P – gas pressure, MPa.
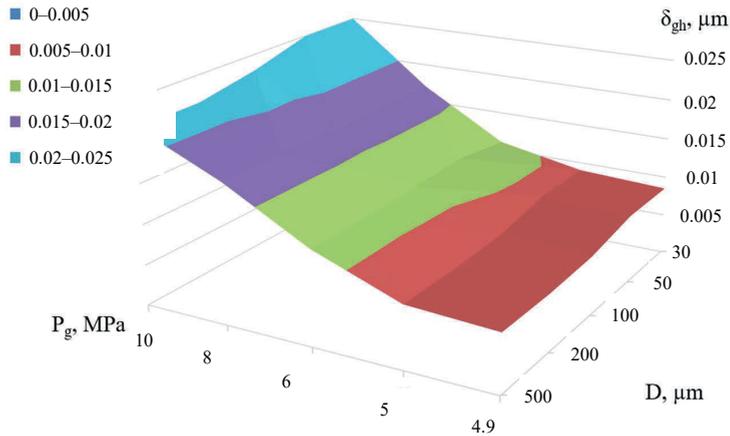
Fig. 9. The thickness of the GH crust (δ_{gh}) depending on the gas pressure (P_g) and liquid droplet size (D).

Thus, the calculation results convincingly prove that gas pressure is another intensifying factor of hydrate formation.

6. DISCUSSION OF THE RESULTS OF STUDIES OF THE INTENSITY OF HYDRATE FORMATION ON THE SURFACE OF THE DROPLET

The calculation results show that the main ways of intensification of GH synthesis are: obtaining a finer aerosol, maintaining the gas temperature at the level of 0 °C, and increasing the gas pressure. If we combine the influence of the above factors, we will get an equation for determining the relative volume of synthesized GH

$$\overline{V}_{gh} = \frac{V_{gh}}{V_w} = \frac{\tau^{0.6}\sigma^{0.4868}}{D^{0.941}}(728.2P - 1655), \tag{51}$$

where

V_{gh}	Volume of synthesized GH, m³;
V_w	Volume of water used to obtain GH, m³;
τ	Time, s;
σ	Gas permeability of GH, m²/s;
D	Droplet size, mm;
P	Gas pressure, MPa.

It has been found that the initial phase of droplet acceleration in the gas phase is too short to have a significant effect on the accumulation of gas hydrate. Therefore, nozzles should be used that make it possible to obtain small droplets at minimum gas flow rates. After the formation of droplets, the gas velocity should be reduced to increase the time of hydrogenesis. A constructive solution for the implementation of this process can be a Laval nozzle, which will also reduce the energy consumption for dispersion. It is also possible to spray water in a stationary gas environment.

Mathematical modelling of hydrate formation showed the promising use of droplets smaller than 100 microns. Reducing the droplet size by half allows to increase the intensity of hydrate formation by two to four times.

Also, the results of mathematical modeling showed that the optimal temperature for hydrate formation is a gas temperature of 0 °C. Deviations from this temperature will lead to a sharp decrease in the intensity of hydrate formation. Cooled gas can be obtained relatively simply in the process of throttling it.

The study of the effect of the gas permeability of the GH crust on the surface of the droplet showed the need for experimental clarification of this value, since it can reduce the intensity of hydrate formation by approximately ten times.

The calculation results confirmed the thesis that gas pressure is also an important factor in the intensification of hydrate formation. An increase in gas pressure leads to a proportional increase in the amount of gas hydrate. However, for methane, doubling the pressure can lead to a significant increase in the metal capacity of the equipment.

7. CONCLUSIONS

Thus, as a result of mathematical modelling of the process of synthesis of methane hydrate on the surface of a droplet of water moving in a gas flow, quantitative dependencies have been established that take into account the influence of such factors as the size of liquid drops; different mutual velocities of gas and drop; time; gas pressures and temperatures; gas permeability of GH. Approximation formulas were obtained that characterizes the influence of these factors and allows predicting the intensity of hydrate formation in injection-type installations.

8. PLANS

The obtained results create the basis for a purposeful selection of spraying equipment for the industrial synthesis of gas hydrates and optimization of its operation modes. It is also worth comparing the obtained results with the rate of hydrate formation on the surface of gas bubbles. This will make it possible to find out the most promising mechanism for the synthesis of gas hydrates.

REFERENCES

[1] Koh C. A., *et al.* State of the art: Natural gas hydrates as a natural resource. *J. Nat. Gas Sci. Eng*. 2012:8:132–138. https://doi.org/10.1016/j.jngse.2012.01.005

[2] Pavlenko A. M. Self-preservation Effect of Gas Hydrates. *Roc. Och. Srod.* 2021:23:346–355. https://doi.org/10.54740/ros.2021.023

[3] Boswell R., *et al.* 6 - Natural Gas Hydrates: Status of Potential as an Energy Resource. Future Energy (Third Edition). Sustainable and Clean Options for our Planet. Elsevier, 2020:111–131. https://doi.org/10.1016/B978-0-08-102886-5.00006-2

[4] Boswell R., Collett T. S. Current perspectives on gas hydrate resources. *En. Env. Sci*. 2011:4:1045–1528. https://doi.org/10.1039/C0EE00203H

[5] Zhao J., *et al.* Analyzing the process of gas production for natural gas hydrate using depressurization. *Appl. En.* 2015:142:125–134. https://doi.org/10.1016/j.apenergy.2014.12.071

[6] Kiran B. S., *et al.* Experimental investigations on tetrahydrofuran-methanewater system: Rapid methane gas storage in hydrates. *Oil Gas Sci. Technol.-Rev. IFP Energ. Nouv*. 2019:74:12. https://doi.org/10.2516/ogst/2018092

[7] Pavlenko A. M. Thermodynamic Features of the Intensive Formation of Hydrocarbon Hydrates. *Energies* 2020:13(13):3396. https://doi.org/10.3390/en13133396

[8] Veluswamy H. P., *et al.* An innovative approach to enhance methane hydrate formation kinetics with leucine for energy storage application. *Appl. En.* 2017:188:190–199. https://doi.org/10.1016/j.apenergy.2016.12.002

[9] Pavlenko A. M., Koshlak H. Application of thermal and cavitation effects for heat and mass transfer process intensification in multicomponent liquid media. *Energies* 2021:14(23):7996. https://doi.org/10.3390/en14237996

[10] Kutnyi B. A. Thermodynamic basis of synthesis of gas hydrates: monograph (Termodynamichni osnovy syntezu hazovykh hidrativ: monohrafiia.). Ivano-Frankivsk: Vydavnytstvo IFNTUNH, 2019. (in Ukrainian)

[11] Sowjanya Y., Prasad P. S. R. Formation kinetics & phase stability of double hydrates of C4H8O and CO2/CH4: A comparison with pure systems. *J. Nat. Gas Sc. Eng.* 2014:18:58–63. https://doi.org/10.1016/j.jngse.2014.02.001

[12] Koshlak, H., Pavlenko, A. Method of formation of thermophysical properties of porous materials. *Roc. Och. Srod.* 2019:21(2):1253–1262.

[13] Delahaye A., *et al.* Effect of THF on equilibrium pressure and dissociation enthalpy of CO_2 hydrates applied to secondary refrigeration. *Ind. Eng. Chem. Res.* 2006:45(1):391–397. https://doi.org/10.1021/ie050356p

[14] Lang X., Fan S., Wang Y. Intensification of methane and hydrogen storage in clathrate hydrate and future prospect. *J. Nat. Gas Chem.* 2010:19(3):203–209. https://doi.org/10.1016/S1003-9953(09)60079-7

[15] Pavlenko A. M. Energy conversion in heat and mass transfer processes in boiling emulsions. *Therm. Scien. Eng. Prog.* 2019:15:100439. https://doi.org/10.1016/j.tsep.2019.100439

[16] Liu Y., *et al.* Methane storage in a hydrated form as promoted by leucines for possible application to natural gas transportation and storage. *En. Tech.* 2015:3(8):815–819. https://doi.org/10.1002/ente.201500048

[17] Xu H., *et al.* Decomposition characteristics of natural gas hydrates in hydraulic lifting pipelines. *Nat. Gas Ind. B* 2019:6(2):159–167. https://doi.org/10.1016/j.ngib.2018.07.005

[18] Zhou X., *et al.* Recyclable and efficient hydrate-based CH_4 storage strengthened by fabrics. *Appl. En.* 2023:336:120820. https://doi.org/10.1016/j.apenergy.2023.120820

[19] Pavlenko A. M., Koshlak H. Production of porous material with projected thermophysical characteristics. *Metal. Min. Ind.* 2015:7(1):123–127.

[20] Liu Z., *et al.* Study on the characteristics of hydrate formation in HSB solution: Focused on the micro-morphologies. *Energy* 2022:244(B):123149. https://doi.org/10.1016/j.energy.2022.123149

[21] Veluswamy H. P., *et al.* A review of solidified natural gas (SNG) technology for gas storage via clathrate hydrates. *Appl. En.* 2018:216(C):262–285. https://doi.org/10.1016/j.apenergy.2018.02.059

[22] Pahlavanzadeh H., *et al.* Gas Hydrate Phase Equilibrium Data for the CO2 + TBPB + THF + Water System. *J. Chem. Eng. Data* 2022:67(9):2792–2799. https://doi.org/10.1021/acs.jced.2c00282

[23] Jin Y., *et al.* Growth of methane clathrate hydrates in porous media. *Energ. Fuel* 2012:26(4):2242–2247. https://doi.org/10.1021/ef3001357

[24] Siazik J., Malcho M. Accumulation of primary energy into natural gas hydrates. *Proc. Eng.* 2017:192:782–787. https://doi.org/10.1016/j.proeng.2017.06.135

[25] Nguyen N. N., *et al.* "Liquid-like" Water in Clathrates Induced by Host–Guest Hydrogen Bonding. *J. Phys. Chem. C* 2021:125(28):15751–15757. https://doi.org/10.1021/acs.jpcc.1c05531

[26] Pavlenko A. M., Koshlak H. A New Method for the Rapid Synthesis of Gas Hydrates for their Storage and Transportation. *Env. Clim. Tech.* 2022:26(1):199–212. https://doi.org/10.2478/rtuect-2022-0016